HHS Public Access

Author manuscript

Prog Biophys Mol Biol. Author manuscript; available in PMC 2017 January 01.

Published in final edited form as:

Prog Biophys Mol Biol. 2016 January ; 120(1-3): 270–280. doi:10.1016/j.pbiomolbio.2015.12.012.

Rate-dependent force, intracellular calcium, and action potential voltage alternans are modulated by sarcomere length and heart failure induced-remodeling of thin filament regulation in human heart failure: A myocyte modeling study

Melanie A. Zile[a] and **Natalia A. Trayanova**[b]

Melanie A. Zile: mzile@jhu.edu; Natalia A. Trayanova: ntrayan1@jhu.edu

a

b

Abstract

Microvolt T-wave alternans (MTWA) testing identifies heart failure patients at risk for lethal ventricular arrhythmias at near-resting heart rates (<110 beats per minute). Since pressure alternans occurs simultaneously with MTWA and has a higher signal to noise ratio, it may be a better predictor of arrhythmia, although the mechanism remains unknown. Therefore, we investigated the relationship between force alternans (FORCE-ALT), the cellular manifestation of pressure alternans, and APV-ALT, the cellular driver of MTWA. Our goal was to uncover the mechanisms linking APV-ALT and FORCE-ALT in failing human myocytes and to investigate how the link between those alternans was affected by pacing rate and by physiological conditions such as sarcomere length and heart failure induced-remodeling of mechanical parameters. To achieve this, a mechanically-based, strongly coupled human electromechanical myocyte model was constructed. Reducing the sarcoplasmic reticulum calcium uptake current (I_{up}) to 27% was incorporated to simulate abnormal calcium handling in human heart failure. Mechanical remodeling was incorporated to simulate altered thin filament activation and crossbridge (XB) cycling rates. A dynamical pacing protocol was used to investigate the development of intracellular calcium concentration ($[Ca]_i$), voltage, and active force alternans at different pacing rates. FORCE-ALT only occurred in simulations incorporating reduced I_{up}, demonstrating that alternans in the intracellular calcium concentration (CA-ALT) induced FORCE-ALT. The magnitude of FORCE-ALT was found to be largest at clinically relevant pacing rates (<110 bpm), where APV-ALT was smallest. We found that the magnitudes of FORCE-ALT, CA-ALT and APV-ALT were altered by heart failure induced-remodeling of mechanical parameters and sarcomere length due to the presence of myofilament feedback. These findings provide important insight into the relationship between heart-failure-induced electrical and mechanical alternans and how they are altered by physiological conditions at near-resting heart rates.

Correspondence to: Natalia A. Trayanova, ntrayan1@jhu.edu.

Keywords

force alternans; action potential alternans; pressure alternans; heart failure; computer modeling

1. Introduction

Ventricular arrhythmias are the most common cause of sudden cardiac death, resulting in > 300,000 US deaths annually (Lloyd-Jones et al., 2009). The standard procedure for preventing sudden cardiac death is to implant a cardioverter defibrillator (ICD), which delivers a strong electric shock to terminate arrhythmias. Since current methods for identifying patients who require ICDs have only been partially successful (Bardy et al., 2005), there is a need for noninvasive predictors with high sensitivity and specificity. Indeed, robust methods for stratifying the risk of lethal cardiac arrhythmias would decrease morbidity and mortality in patients with cardiovascular disease and reduce health care costs (Goldberger et al., 2011). Approaches for stratifying risk of cardiac arrhythmias involve testing for abnormalities in the ECG, then using the results to identify patients who would benefit from ICD therapy. ECG-based risk stratification methods scan for abnormalities in ventricular depolarization (late potentials (Kuchar et al., 1987), fractionated QRS complexes (Das et al., 2006)) and repolarization (T-wave alternans (Rosenbaum et al., 1994), and QT variability, dispersion, and instability (Berger et al., 1997; Chen et al., 2011; Chen et al., 2013; Chen and Trayanova, 2012; Couderc et al., 2007)). However, the mechanisms underlying these ECG indices, and their relationship to lethal cardiac arrhythmias, are not fully understood. This lack of knowledge likely explains why results of clinical trials to correlate surface EGG indices to lethal cardiac arrhythmias are often contradictory (Goldberger et al., 2011).

Of the above ECG indices, T-wave alternans have received possibly the most attention. Research has reported a strong correlation between increased arrhythmia risk and the presence of T-wave alternans (Narayan, 2006; Qu et al., 2010), defined as the beat-to-beat alternation of the timing or shape of the repolarization wave of the ECG. In the clinical setting, testing for Microvolt T-wave Alternans (MTWA) has been found to be a risk marker for lethal ventricular arrhythmias and sudden cardiac death (Cutler and Rosenbaum, 2009), to have high negative predictive power (Narayan, 2006) and to be particularly promising in dichotomizing patients that would and would not benefit from ICD therapy (Bloomfield et al., 2006; Hohnloser et al., 2009). However, the mechanistic basis of MTWA preceding lethal ventricular arrhythmias has long been under debate. Until the last decade, it was believed that a steep action potential duration (APD) restitution (>1) at rapid heart rates (Weiss et al., 2006) produces alternans in APD that underlie T-wave alternans and the genesis of fibrillation (Pastore et al., 1999). However, MTWA is most successful in stratifying risk in patients at near-resting heart rates <110 bpm, where APD restitution is flat (Narayan et al., 2007). Computational models of the LV wall in combination with clinical data revealed that abnormal handing of intracellular calcium underlies alternans in action potential voltage (APV-ALT), defined as the oscillation of the plateau voltage of the action potential, which results in MTWA at moderate heart rates, i.e. <110 bpm (Bayer et al., 2010;

Narayan et al., 2008). Thus APV-ALT is the cell-level driver of MTWA at these rates under the conditions of heart failure.

Alternatively, noninvasively measured pressure alternans, defined as the beat-to-beat oscillation of the amplitude of systolic pressure, has been found to be a predictor of worsening heart failure and increased cardiac mortality (Hirashiki et al., 2010; Hirashiki et al., 2006; Ito et al., 2012; Kashimura et al., 2014; Kim et al., 2014; Selvaraj et al., 2011). Pressure alternans also occurs simultaneously with MTWA in patients at near resting heart rates, thus indicating that pressure alternans, which have higher signal-to-noise ratio (Selvaraj et al., 2011), may be a better predictor of the propensity for ventricular arrhythmias and sudden cardiac death, however the mechanisms remain unknown.

At the cellular level, pressure alternans arise from force alternans (FORCE-ALT), defined as the beat-to-beat oscillations in the strength of active force production in cardiac muscle. APV-ALT at heart rates <110 bpm has been found to be driven by beat-to-beat fluctuations in the amplitude of the intracellular calcium concentration (CA-ALT) (Bayer et al., 2010; Narayan et al., 2008). CA-ALT has also been shown to underlie force alternans (FORCE-ALT), in animal experiments with cardiac muscle preparations (Kihara and Morgan, 1991; Kotsanas et al., 1996; Lab and Lee, 1990; Orchard et al., 1991) and perfused hearts (Brooks et al., 1994; Lee et al., 1988), but only at fast pacing rates. Clearly, to date, no studies have investigated FORCE-ALT in human myocytes at rates <110 bpm, and although calcium dysregulation is a likely candidate, the exact mechanistic link between APV-ALT and FORCE-ALT in the failing human myocyte at the clinically important near-resting heart rates remains unknown. Therefore, our goal was to investigate the mechanisms linking FORCE-ALT to APV-ALT in the human failing myocyte, with emphasis on those acting at the clinically-relevant pacing rates of <110 bpm, and to uncover how the link between FORCE-ALT and APV-ALT is affected by various physiological conditions such as sarcomere length and heart failure induced-remodeling of mechanical parameters.

2. Methods

2.1. Human Electromechanical Myocyte Model

To uncover the mechanism linking FORCE-ALT to APV-ALT, a mechanistically-based human electromechanical myocyte model was used. The electromechanical model combined the human endocardial ventricular membrane kinetics model by ten Tusscher *et al* (ten Tusscher and Panfilov, 2006) and the myofilament dynamics model by Rice *et al* (Rice et al., 2008). The 2006 ten Tusscher *et al* formulation was used because it incorporated an extensive description of intracellular calcium handling, which was found to be critical in the development of APV-ALT in previous studies of human heart failure (Bayer et al., 2010; Narayan et al., 2008). The Rice *et al* model, which describes the activation of the thin filament by intracellular calcium binding to Troponin C as well as thin filament binding to thick filament crossbridges (XBs) using a 5 state Markov model, was chosen because it was computationally efficient while incorporating important biophysical detail and cooperativity mechanisms. Since the Rice *et al* myofilament model was developed based on rabbit data we adjusted it to match human force data. This was done by modifying XB cycling and calcium-based thin filament activation parameters following the approach in de Oliveira *et*

al (de Oliveira et al., 2013). To account for the differences between the ionic model used by de Oliveira *et al* (the 2004 formulation of the ten Tusscher *et al* model (ten Tusscher et al., 2004)) and by us (ten Tusscher and Panfilov, 2006), additional modifications to calcium-based thin filament activation were made. Specifically, we decreased thin filament activation by reducing k_{on}, a parameter regulating the binding affinity of Ca to high and low regulatory sites on Troponin C, to 95% of the baseline value used in Rice *et al*, in order to increase the time to peak force value so that it fell in the physiological range of human values (Mulieri et al., 1992; Pieske et al., 1996).

The ionic and myofilament models were strongly coupled by incorporating myofilament feedback on calcium dynamics (Figure 1); this was done by incorporating a dynamic term for troponin buffering of intracellular calcium ($[Ca]_{Troponin}$) using the approach in Rice *et al*. Strongly coupling the models with a dynamic representation of $[Ca]_{Troponin}$ was important and necessary, because it has been shown to be crucial for accurately reproducing contractile experiment data in myocyte simulations (Ji et al., 2015). This $[Ca]_{Troponin}$ term represents the amount of calcium bound to troponin and incorporates the cooperativity of calcium-troponin binding due to strongly bound nearby XBs. However, in the 2006 ten Tusscher and Panfilov model, troponin buffering of calcium is combined with calmodulin buffering of calcium and is represented using a steady state approximation. Therefore, to incorporate feedback from the myofilament model to the ionic model, we separated the combined buffering term in ten Tusscher and Panfilov into two terms. The $[Ca]_{Troponin}$ term from Rice *et al*, calculated using ordinary differential equations, was used for troponin buffering of calcium, and a steady state approximation was used for calmodulin buffering of calcium ($[Ca]_{Calmodulin}$) using the same approach as de Oliveira *et al*. The following equation from de Oliveira *et al* was used to update the intracellular calcium concentration in the ionic model, using the $[Ca]_{Troponin}$ term calculated by the myofilament model, at each time step:

$$[Ca]_{Total} = [Ca]_i + [Ca]_{Calmodulin} + [Ca]_{Troponin} \quad (1)$$

where $[Ca]_{Total}$ is the total calcium in the cytoplasm, $[Ca]_i$ is the free calcium in the cytoplasm, $[Ca]_{Calmodulin}$ is the total calcium buffered by calmodulin in the cytoplasm, and $[Ca]_{Troponin}$ is the total calcium bound to Troponin C.

A weakly coupled version of the model (with no feedback) was created by removing the $[Ca]_{Troponin}$ term from Equation 1. Its sole purpose was to aid in examining how myofilament feedback affected the development of alternans.

The model did not incorporate stretch-activated channels since there is no experimental evidence that heart-failure induced APV-ALT at low heart rates would be affected by a potential opening of the channel.

2.2. Incorporating Heart Failure Remodeling

We simulated human heart failure in our electromechanical model by incorporating electrical and mechanical remodeling. Electrical remodeling was represented by abnormal calcium handing. Specifically, we reduced the sarcoplasmic reticulum calcium uptake current (I_{up}) to 27% of its baseline value in the ten Tusscher *et al* model (Table 1), similar to

Narayan *et al* (Narayan et al., 2008) and Bayer *et al* (Bayer et al., 2010), to represent reduced SERCA2a expression (Hasenfuss et al., 1994) and increased dephosphorylated phospholamban (Schmidt et al., 1999) observed in human heart failure. This specific feature of heart failure remodeling was incorporated because it has been shown to be crucial to the development of APV-ALT in previous studies of human heart failure (Bayer et al., 2010; Narayan et al., 2008).

Mechanical remodeling was incorporated to simulate altered thin filament activation and XB cycling rates found in human heart failure. Changes in thin filament activation have been linked to altered phosphorylation of cardiac Troponin I (cTnI) (Messer et al., 2007), which has been shown to be decreased by up to 87% (Messer et al., 2007; Zaremba et al., 2007). Alterations in XB cycling rates have been linked to changes in phosphorylation of myosin light chain 2 (MLC-2) (Levine et al., 1996; Moss and Fitzsimons, 2006; Olsson et al., 2004; Patel et al., 1998) and cardiac myosin-binding protein C (cMyBP-C) (Coulton and Stelzer, 2012; Flashman et al., 2004). Studies have found that phosphorylation of the two isoforms of MLC-2 is unchanged (van der Velden et al., 2003a) or reduced by 34%-69% (van Der Velden et al., 2001; van der Velden et al., 2003a; van der Velden et al., 2003b; Zaremba et al., 2007). Additionally, cMyBP-C has been shown to be decreased by at least 50% (El-Armouche et al., 2007; Zaremba et al., 2007). Furthermore, myocardial Ca^{2+} sensitivity, which incorporates the combination of the effects of thin filament activation and XB cycling rates on force production, has been shown to be altered in human heart failure. In studies, myocardial Ca^{2+} sensitivity has been found to increase by 2–6% in human heart failure (van der Velden et al., 2000; van der Velden et al., 2006; Wolff et al., 1996) and by 1–2% in animal models of heart failure (de Waard et al., 2007; Lamberts et al., 2007; Wolff et al., 1995), not change in human heart failure (Ambardekar et al., 2011), and decrease by 2–3% in animal models of heart failure (Belin et al., 2007; Belin et al., 2006).

Despite the uncertainty regarding the exact amount by which the mechanical properties outlined above are altered in heart failure, these studies indicate that mechanical parameters involved in thin filament activation and XB cycling are important components of the disease manifestation and therefore might contribute to the development of FORCE-ALT. To elucidate if and how changes to mechanical parameters in human heart failure promote or modulate FORCE-ALT, we incorporated mechanical remodeling into the Rice *et al* myofilament model. Specifically, we altered thin filament activation, embodied in the Rice *et al* model by these 6 parameters: $perm_{50}$, k_{offL}, k_{offH}, k_{on}, k_{n_p}, and k_{p_n}. k_{npT} and k_{pnT} are nonlinear transition rates that are functions of these 6 parameters and represent calcium based activation of the thin filament, which is shown in Figure 1 as the transition of the thin filament from the N_{XB} state (XB formation is inhibited) to the P_{XB} state (weakly bound XB formation is possible). Specifically, $perm_{50}$ is the half activation constant for shift of a thin filament regulatory unit (RU) from N_{XB} to P_{XB}, k_{offH} (k_{offL}) is the rate constant for Ca^{2+} unbinding from the high (low) affinity binding site of Troponin C, and k_{on} is rate constant for Ca^{2+} binding to Troponin C. k_{n_p} and k_{p_n} are constant scaling factors of the k_{npT} and k_{pnT} transition rates. We also altered XB cycling rates, expressed by these Rice *et al* parameters: f_{app}, g_{app}, h_f, h_b, and g_{xb}. The rates fapp and gapp regulate the transition of the thin filament from the P_{XB} state to the strongly bound XB state where the myosin head has

not yet rotated and induced strain in the neck region (XB_{PreR}). h_f and h_b are transition rates between the XB_{PreR} and XB_{PostR} state (thin filament is strongly bound to a XB which has a rotated myosin head and has induced distortion). g_{xb} represents the ATP consuming transition rate from XB_{PostR} to P_{XB}. Due to the uncertainty in the literature regarding the exact amount that these parameters change in heart failure, as described above, we explored heart failure –induced remodeling of these 11 myofilament parameters within the range of 80% to 120% of their baseline values (Table 1).

2.3. Alternans Protocol

Clinical studies in patients with human heart failure have shown that APV-ALT arises at moderate pacing rates (Narayan et al., 2008); APV-ALT has also been induced, at these rates, in computational electrophysiological models of human myocytes and LV wedges with abnormal calcium handing by pacing the models with a dynamic pacing protocol (Bayer et al., 2010). To induce APV-ALT in our electromechanical model of the myocyte, we used a pacing protocol similar to that in Bayer *et al*. (Bayer et al., 2010). We first paced the myocyte at near resting pacing rates (850 ms; 71 bpm) until steady state was reached. Then, a dynamic pacing protocol was executed with pacing beginning at a cycle length (CL) of 650 ms (92 bpm) and decreasing by 50 ms every 100 beats, until loss of 1:1 capture occurred.

Since our myocyte model is a strongly coupled electromechanical model, the procedure used to induce APV-ALT was also expected to result in the generation of FORCE-ALT. We aimed to test this hypothesis and to uncover the mechanism linking FORCE-ALT to APV-ALT. The pacing protocol also allowed us to probe the sensitivity of FORCE-ALT to CL.

To elucidate if altered thin filament activation and XB cycling rates found in human heart failure exacerbated or alleviated FORCE-ALT, we examined how each remodeled parameter described above individually affected FORCE-ALT; 11 sets of simulations were thus run using the dynamic pacing protocol, each including the electrical remodeling and the remodeling of one of the myofilament parameters. To uncover the effect of disease severity for each remodeled myofilament parameter, each set of simulations consisted of 41 unique simulations in which the chosen mechanical parameter was assigned a value in the range of 80% to 120% of its baseline value in Rice *et al* (incremented by 1%). To discover if FORCE-ALT can be induced by mechanical remodeling and dynamic pacing alone, the 451 simulations just described were executed again but without the inclusion of electrical remodeling.

Finally, since active force generation is known to be modulated by sarcomere length (SL) (Gordon et al., 1966), we wanted to uncover if FORCE-ALT was also sensitive to SL. To do this, the aforementioned 451 simulations (with the electrical remodeling) were each run 16 times, during which we held SL constant at a different value for each simulation. SL values ranged from 1.65 μm to 2.4 μm, in increments of 0.05 μm. This range of SL values was chosen because it is in the operating range for cardiac myocytes (Trayanova and Rice, 2011).

2.4. Alternans Analysis

The magnitudes of alternans in active force, intracellular calcium concentration ($[Ca]_i$), and transmembrane voltage (V_m) were each calculated using the following formula commonly used in the quantification of alternans (Kockskamper and Blatter, 2002; Shkryl et al., 2012; Xie et al., 2013):

$$ALTM = 1 - \frac{Small\ Amplitude}{Large\ Amplitude} \quad (2)$$

where *Small Amplitude* is the peak value minus the minimum value during the small beat and *Large Amplitude* is the peak value minus the minimum value during the large beat. Alternans magnitude was calculated for each pair of beats during the final 64 beats of each CL, following the approach in Bayer *et al* (Bayer et al., 2010) and the largest alternans magnitude per CL for each simulation was recorded. APV-ALT was calculated, as described above, during the period from the start of Phase II until the end of Phase III of the action potential. Alternans occurred if ALT > 0.

3. Results

3.1. Abnormal Intracellular Calcium Handling Results in Force Alternans

Incorporating heart failure electrical remodeling in our strongly coupled cellular electromechanical model (as described in Methods) resulted, as expected, in intracellular calcium alternans (CA-ALT) that caused action potential voltage alternans (APV-ALT), similar to those shown previously (Bayer et al., 2010; Narayan et al., 2008). An example of CA-ALT as a function of time and as superimposed beats is shown in Figure 2, panels A and E respectively, for pacing at a CL of 650 ms (92 bpm) and for a SL of 2.1 μm (a typical length during the normal cardiac cycle). The superimposed beats emphasize the presence of CA-ALT and the difference in the Ca^{2+} transient between the odd (small $[Ca]_i$ transient) and even (large $[Ca]_i$ transient) beats. The corresponding APV-ALT is shown in Figure 2, panels B and F. CA-ALT also induced alternans in active force (FORCE-ALT), shown as a function of time (Figure 2C) and as overlaid beats (Figure 2H).

Due to myofilament feedback in our strongly coupled model (Figure 2, panels C and G), CA-ALT and APV-ALT differed from those obtained by Bayer et al and Narayan et al (Bayer et al., 2010; Narayan et al., 2008). We used the weakly coupled version of the model to explore the effects of myofilament feedback on CA-ALT, APV-ALT, and FORCE-ALT (compare rows 2 and 3 of Figure 2). The magnitudes of $[Ca]_i$ and CA-ALT (CA-ALTM) were both smaller in the strongly coupled model as compared to those in the weakly coupled ($[Ca]_i$: 0.44 μM vs 0.50 μM for odd beat, 0.51 μM vs 0.68 μM for even beat; CA-ALTM: 21% vs 35%). Since Troponin C binds free intracellular calcium and thus removes those calcium ions from the pool of free calcium available in the cytoplasm ($[Ca]_i$), the feedback via the $[Ca]_{Troponin}$ term (Equation 1) in the strongly coupled model resulted in a smaller magnitude of $[Ca]_i$. Smaller CA-ALTM was due to the fact that Troponin C buffers more $[Ca]_i$ when $[Ca]_i$ transient is large (even beat) than when it is small (odd beat), thus reducing the peak magnitude of $[Ca]_i$ during the even beat relative to that of the odd and consequently decreasing CA-ALTM, as calculated according to Equation 2. The magnitude of APV-ALT

(APV-ALTM) was also smaller in the strongly coupled model (46% vs. 68% with no feedback) due to diminished CA-ALTM. The magnitude of $[Ca]_{Troponin}$ was smaller in the strongly vs weakly coupled model ($[Ca]_{Troponin}$: 8.73 μM vs 13.19 μM for odd beat, 14.86 μM vs 24.17 μM for even beat) due to diminished $[Ca]_i$. The strong coupling also resulted in a smaller magnitude of the active force due to the decreased $[Ca]_i$ transient (0.18 vs 0.36 normalized force for odd beat, 0.46 vs 0.79 for even beat). However, the magnitude of FORCE-ALT (FORCE-ALTM) was 5% greater in the case of myofilament feedback than without (60% vs. 55%), despite the smaller CA-ALTM in the former case. This was due to a smaller amount of calcium bound to Troponin C during both the odd and even beats, resulting from the reduced $[Ca]_i$ in this case. Since calcium binding to Troponin C activates the thin filament, less thin filament regulatory units (RUs) transitioned from the non-permissive (N_{XB}; XB formation is inhibited) to the permissive (P_{XB}; weakly-bound XBs formation possible) state, (Figure 1) resulting in less RUs transitioning from P_{XB} to the states with strongly-bound XBs (XB_{PreR} and XB_{PostR}). Since active force is generated by the rotation of the thick filament, fewer RUs in the pre-rotated (XB_{PreR}) state caused less RUs to transition from it to the post-rotated (XB_{PostR}) state, producing less active force. However, since the presence of strongly bound XBs is known to enhance the binding affinity of Troponin C to calcium on nearby thin filament RUs and since Rice et al (Rice et al., 2008) incorporated this nonlinear cooperativity mechanism, the relatively smaller amount of strongly bound XBs during the odd (smaller $[Ca]_i$) beat resulted in greater reduction of active force generation relative to the even (larger $[Ca]_i$) beat. This resulted in enhanced FORCE-ALTM in the strongly coupled model as calculated according to Equation 2.

3.2. Sensitivity of Alternans to Pacing Rate

Simulations with our strongly coupled electromechanical myocyte model revealed that FORCE-ALTM has a non-monotonic dependence on CL (Figure 3A, solid line), with a local minimum at CL=400 ms. CA-ALTM monotonically increased with increased pacing rate, while APV-ALTM remained relatively small at slower pacing rates and increased at faster pacing rates (Figure 3B–C, solid line). No alternans occurred for pacing CLs>650 ms. An important observation here is that for all clinically relevant pacing rates (as discussed in the Introduction, <110 bpm; CL>=550 ms), CA-ALTM, ranging 21%-31%, induced smaller APV-ALTM (ranging 46–48%) but larger FORCE-ALTM (ranging 51–61%), consistent with the results presented in Figure 2. However, at faster pacing rates (CL<500 ms), larger CA-ALTM induced smaller FORCE-ALTM. This was due to elevated $[Ca]_i$, which occurred due to a buildup of diastolic intracellular calcium as a result of insufficient time between beats for the SERCA pump and the Na/Ca^{2+} exchanger to restore $[Ca]_i$ to normal. During the large (even) beat, this abnormally large $[Ca]_i$ transient saturated Troponin C prior to reaching its peak magnitude, preventing additional free calcium from binding to Troponin C and thus preventing an increase in thin filament activation. This prevented further thin filament RUs from transitioning to the P_{XB}, XB_{PreR} and XB_{PostR} states from the N_{XB} state (Figure 1). Since no additional rotation of the thick filament occurred, no added active force was generated during the even beat, despite additional free calcium becoming available as the $[Ca]_i$ transient increased from the value at which Troponin C saturated to its peak

magnitude. This resulted in diminished FORCE-ALTM at faster pacing rates, according to Equation 2.

Eliminating myofilament feedback reduced FORCE-ALTM at all CLs on average by 11%, flattened the CA-ALTM dependence, and increased APV-ALTM (Figure 3A–C, dashed line), rendering the latter similar to the dependence documented by Bayer *et al* and Narayan *et al* (Bayer et al., 2010; Narayan et al., 2008). CA-ALTM was smaller for the strongly verses the weakly coupled model at slower pacing rates (CL>450 ms), consistent with the results presented in Section 3.1 for CL=650 ms (Figure 2). However, CA-ALTM became larger than that for the weakly coupled model at faster pacing rates (CL<400 ms) due to diminished myofilament feedback during the even but not the odd beat. As CL decreased, $[Ca]_i$, was elevated and saturated Troponin C during the even beat, preventing both additional free calcium from binding to Troponin C, and additional thin filament RUs from transitioning from the N_{XB} to the P_{XB} and strongly-bound XB states, as discussed in the preceding paragraph. Since $[Ca]_{Troponin}$ is a function of the amount of calcium bound to Troponin C and of the number of RUs in the strongly-bound XB states, myofilament feedback was diminished during the even beat more than the odd, thus reducing the magnitude of $[Ca]_i$ more during the odd beat. This resulted in larger CA-ALTM for the strongly coupled model at faster rates.

3.3. Dependence of Force, Calcium and Voltage Alternans on Sarcomere Length

Simulations with our strongly coupled electromechanical myocyte model showed that, alternans magnitude changed as SL decreased from 2.4 to 1.65 μm. An example of the dependence of the three types of alternans magnitude on SL functions for pacing at a CL of 600 ms (100 bpm) is shown in Figure 4A–C, solid line. CA-ALTM increased for SL>2.05 μm (in Figure 4B) due to diminished myofilament feedback during the even beat only, which occurred as a result of a progressive increase in the fraction of single-overlap thin filament apposing the thick filament as SL increased. Since this portion of the thin filament has a higher binding affinity to calcium, a larger fraction of it caused greater calcium-Troponin C binding for a given $[Ca]_i$. This progressively lowered the $[Ca]_i$ threshold at which Troponin C became saturated, preventing additional free calcium from binding to Troponin C, despite the peak magnitude of the $[Ca]_i$ transient being greater than the $[Ca]_i$ threshold for saturation. This saturation only occurred during the even beat due to its larger $[Ca]_i$ magnitude. Since $[Ca]_{Troponin}$ is a function of the amount of calcium bound to Troponin C, myofilament feedback was increasingly diminished at progressively larger SLs during the even beat relative to the odd, thus steadily reducing the magnitude of $[Ca]_i$ during the even beat (according to Equation 1). This resulted in progressively larger CA-ALTM, according to Equation 2, at increasingly greater SLs for SL>2.05 μm. The saturation of Troponin C during the even beat also prevented enhanced thin filament activation, which, as described in Section 3.2., resulted in progressively diminished FORCE-ALTM, as shown for SL increasing above 2.05 μm in Figure 4A. APV-ALTM decreased for SL>2.05 μm, despite increased CA-ALTM, due to increasingly diminished $[Ca]_{Troponin}$ during the even beat (as described above), which caused the $[Ca]_i$ transient during the even beat to have a notched appearance similar to Figure 2A (red lines). As SL increased, the $[Ca]_i$ magnitude prior to the $[Ca]_i$ notch became increasingly large (due to reduced $[Ca]_{Troponin}$), causing CA-ALTM

to increase in accordance with Equation 1. However, the $[Ca]_i$ transient quickly decreased from the peak value preceding the notch in $[Ca]_i$ to an increasingly smaller value as SL increased, thus shortening Phase II of the action potential and reducing its magnitude during the even beat and inducing smaller APV-ALTM. CA-ALTM also increased for SL<2.05 μm. As SL became progressively smaller, the fraction of single-overlap thin filament that was apposed to thick filament decreased, causing reduced calcium-Troponin C binding for a given $[Ca]_i$. This diminished thin filament activation and decreased the number of RUs that transitioned from N_{XB} to P_{XB}, thus reducing the number of RUs that transitioned to strongly-bound XB states. Since $[Ca]_{Troponin}$ is a function of the amount of calcium bound to Troponin C and of the number of RUs in the strongly-bound XB states, myofilament feedback was progressively diminished during the even relative to the odd beat as SL decreased, thus increasing the magnitude of $[Ca]_i$ more during the even beat. This resulted in progressively larger CA-ALTM as SL decreased for SL<2.05 μm. FORCE-ALTM and APV-ALTM were large at SL<2.05 μm due to large CA-ALM. The trends for CA-ALTM and APV-ALT as functions of SL were different at slow and fast pacing rates (Figure 4E–F), while the dependence of FORCE-ALTM held true at all CLs (Figure 4D).

Eliminating myofilament feedback expanded the range of FORCE-ALTM (Figure 4A, dashed line) without altering the shape of its dependence on SL. As expected, the removal of myofilament feedback rendered CA-ALTM and APV-ALTM insensitive to SL changes (Figure 4B–C, dashed line). FORCE-ALTM was larger in the weakly coupled model at SL<2.0 μm due to larger CA-ALTM; it was smaller at SL>2.0 μm due to enhanced saturation of Troponin C caused by the larger $[Ca]_i$ magnitudes shown to occur in the weakly coupled model (Figure 2I). This resulted in smaller peak active force generation during the even beat and thus diminished FORCE-ALTM (via Equation 2) in the weakly coupled model.

3.4. Effect of Heart Failure Induced-Remodeling of Mechanical Parameters on Force, Calcium and Voltage Alternans

Incorporating heart failure induced-remodeling of both electrical and mechanical parameters in simulations with our strongly coupled electromechanical myocyte model demonstrated that of the mechanical parameters involved in thin filament activation and XB cycling, only remodeling in $perm_{50}$ (half activation constant for shift of a thin filament RU from N_{XB} to P_{XB}), k_{offH} (rate constant for Ca^{2+} unbinding from the high affinity binding site of Troponin C), and k_{on} (rate constant for Ca^{2+} binding to Troponin C) caused appreciable alterations in FORCE-ALTM, CA-ALTM, and APV-ALTM. Of these three, $perm_{50}$ was the most important because changes to it had the most profound effects on FORCE-ALTM, CA-ALTM, and APV-ALTM. Examples of these functions are shown in Figure 5 for $perm_{50}$ (row 1), k_{offH} (row 2), and k_{on} (row 3) for pacing at a CL of 600 ms and SL of 2.1 μm, where each remodeled parameter is displayed as a percent of its normal value. By definition, increasing $perm_{50}$ diminishes thin filament activation. As $perm_{50}$ was progressively increased above 102%, thin filament activation was increasingly reduced, which steadily increased CA-ALTM, FORCE-ALTM and APV-ALTM, via the mechanisms described in Section 3.3 for SL<2.05 μm. As $perm_{50}$ was decreased below 102%, thin filament activation was increasingly enhanced, which increased the transition rate of N_{XB} to P_{XB} and decreased

the reverse rate, causing more RUs to transition to P_{XB}. A greater number of RUs in the P_{XB} state induced additional RUs to transition to the strongly-bound XB states, increasing the fraction of total RUs with strongly-bound XBs. Therefore, achieving the maximum fraction of RUs in the XB_{PreR} and XB_{PostR} states could be attained with increasingly less activating calcium as $perm_{50}$ decreased. Since $[Ca]_{Troponin}$ is a function of the fraction of total RUs in strongly-bound XB states and since during the even beat $[Ca]_i$ was large enough to attain that maximum fraction, myofilament feedback was progressively diminished during the even relative to the odd beat as $perm_{50}$ decreased, thus increasing the magnitude of $[Ca]_i$ more during the even beat. This caused progressively larger CA-ALTM. Active force, which is also a function of the fraction of total RUs in strongly-bound XB states, was progressively diminished during the even verses the odd beat (similar to $[Ca]_{Troponin}$), which resulted in progressively smaller FORCE-ALTM, despite enhanced CA-ALTM, as $perm_{50}$ decreased. APV-ALTM was enhanced due to larger CA-ALTM. By definition, a decrease in k_{offH} or an increase in k_{on} increases the binding affinity of Troponin C to calcium. As k_{offH} was progressively decreased below 103% and k_{on} increased above 92%, binding affinity was increased (thus enhancing calcium-Troponin C binding for a given $[Ca]_i$), which progressively enhanced CA-ALTM and diminished FORCE-ALTM and APV-ALTM, in the same manner as described in Section 3.3. for SL>2.05 μm. k_{offH}>103% and k_{on}<92% decreased the binding affinity of Troponin (thus diminishing thin filament activation), which progressively increased CA-ALTM, FORCE-ALTM and APV-ALTM as described in Section 3.3 for SL<2.05 μm. Removing myofilament feedback decreased FORCE-ALTM for nearly all values of $perm_{50}$, k_{offH}, and k_{on} (Figure 5, column 1, dashed line), and as expected, rendered CA-ALTM and APV-ALTM insensitive to remodeling of those mechanical parameters. FORCE-ALTM was diminished due to enhanced saturation of Troponin C caused by the larger $[Ca]_i$ magnitudes occurring in the weakly coupled model (Figure 2I) in the same manner as described for SL>2.0 μm in Section 3.3.

Finally, simulations were run incorporating only mechanical remodeling (no electrical remodeling). For all CLs and SLs studied, there was no FORCE-ALT, demonstrating that abnormal intracellular calcium handling and thus CA-ALT was necessary for the generation of FORCE-ALT.

4. Discussion

The present study examines the cellular mechanisms underlying the formation of pressure alternans (FORCE-ALT) in the presence of MTWA (APV-ALT), which have been shown to be predictors of worsening heart failure and lethal ventricular arrhythmias, respectively. The goals of this study were to uncover the mechanisms linking APV-ALT and FORCE-ALT in failing human myocytes and to investigate how the link between those alternans was affected by pacing rate and various physiological conditions. Using a strongly coupled human electromechanical myocyte model, we showed that CA-ALT, induced by decreased I_{up}, was the link between APV-ALT and FORCE-ALT and that FORCE-ALTM was largest at clinically-relevant slow to moderate pacing rates (<110 bpm), where APV-ALT was smallest. We found that FORCE-ALTM, CA-ALTM and APV-ALTM were altered by heart failure induced-remodeling of mechanical parameters and by sarcomere length; this was due to the presence of myofilament feedback. Together these findings link FORCE-ALT to

APV-ALT and suggest that pressure alternans is directly linked to MTWA via calcium dysregulation and may be a better predictor of the propensity for ventricular arrhythmias at clinically relevant pacing rates (<110 bpm).

4.1. Calcium Alternans Link Action Potential Voltage Alternans to Force Alternans

MTWA is caused by CA-ALT predominantly as a result of decreased sarcoplasmic reticulum calcium uptake current (I_{up}) in heart failure patients at near resting heart rates (Bayer et al., 2010; Narayan et al., 2008). In addition, MTWA and pressure alternans have been shown to occur simultaneously in patients at such pacing rates (Selvaraj et al., 2011). Furthermore, patients with pressure alternans have significantly lower amounts of sarcoplasmic reticulum Ca^{2+}-ATPase (SERCA) mRNA than patients without (Hirashiki et al., 2010; Hirashiki et al., 2006). Finally, FORCE-ALT, the cellular manifestation of pressure alternans, has been found to be regulated by calcium dysregulation in animal experiments with cardiac muscle preparations (Kihara and Morgan, 1991; Kotsanas et al., 1996; Lab and Lee, 1990; Orchard et al., 1991) and perfused hearts (Brooks et al., 1994; Lee et al., 1988), paced at fast rates. Taken together, the results from these previous studies have suggested that CA-ALT, due to reduced I_{up}, is a likely candidate to underlie FORCE-ALT in human heart failure. Our results presented here provide the proof that CA-ALT, via reduced I_{up}, drove the formation of FORCE-ALT at clinically relevant pacing rates.

4.2. Force Alternans Are Large at Slow Pacing Rates and May Be Undetectable at Faster Pacing Rates

Studies have shown that the mean heart rate onset at which pressure alternans were first detected in pacing studies was 606 ms (99 bpm) (Hirashiki et al., 2006), and 517 to 571 ms (116 bpm – 105 bpm) (Selvaraj et al., 2011). In addition, a study conducted during normal sinus rhythm found that patients with pressure alternans had significantly slower heart rates than those without (81.0 bpm vs 93.1 bpm) (Kim et al., 2014). That same study also showed that patients with both MTWA and pressure alternans had slower heart rates than those with only MTWA (81.0 bpm vs 92 bpm, not statistically significant), suggesting that patients with only MTWA may have had small yet undetectable pressure alternans due to the alternans magnitude being markedly reduced at faster heart rates. One study further supported this hypothesis by showing that the amplitude of pressure alternans declined at increasingly faster pacing rates for four patients, three of whom lost pressure alternans when pacing rates exceeded 120, 130 and 140 bpm (500, 462, 400 ms) respectively (Kashimura et al., 2013). The present study provided support of this finding, since we demonstrated that FORCE-ALTM was greatest at slower pacing rates (>109 bpm) and declined significantly at faster pacing rates (<109 bpm). However, the outcome of one study contradicted these findings and reported that the magnitude of pressure alternans increased from 600 ms to 500 ms (Selvaraj et al., 2011). This conflicting evidence might have arisen from the method of calculating pressure alternans magnitude in that study, which differed from ours (spectral analysis versus measuring the amplitude change between the odd and even beats). To date, few patient studies have investigated the effects of pacing rate on the detection and magnitude of pressure alternans. However, as we have shown, pacing rate affects FORCE-ALTM and could explain why some patients with MTWA do not have detectable pressure alternans despite having underlying abnormal calcium handling. Additional studies of

pressure alternans in heart failure patients are needed to investigate this phenomenon in greater detail.

4.3. Implications of Heart Failure-Induced Mechanical Remodeling for Alternans Severity

Studies have shown that thin filament activation can be altered in human heart failure. Specifically, decreased phosphorylation of cardiac Troponin I has been shown to be significantly decreased in human heart failure (Messer et al., 2007; Zaremba et al., 2007), resulting in reduced sliding speed and an increased Ca2+-sensitivity. Although this change in thin filament activation has been observed in human heart failure, to date no studies have investigated whether it is reduced in patients with pressure alternans or MTWA. Here we demonstrated that heart failure-induced mechanical remodeling of parameters that modify thin filament activation can both exacerbate and diminish FORCE-ALT, CA-ALT, and APV-ALT. These results could explain the results of some studies which have revealed two different populations of patients with alternans: those with both MTWA and pressure alternans and those with only MTWA (Kim et al., 2014; Kodama et al., 2001; Selvaraj et al., 2011). The patient population with both types of alternans could have calcium handling abnormalities and reduced thin filament activation, which would (as our results suggest) result in larger and thus more easily detectable pressure alternans. The patients in which only MTWA were detectable may either have less severe reductions in thin filament activation or no abnormalities at all, and thus have smaller and undetectable pressure alternans. Furthermore, one study has shown that the magnitude of MTWA in patients with both MTWA and pressure alternans is larger than in patients with only MTWA (Kim et al., 2014), suggesting that if those patients had reduced thin filament activation as we speculated, then that would enhance the magnitude of MTWA, in agreement with our results (Figure 5).

5. Conclusions

APV-ALT and FORCE-ALT are linked via CA-ALT, resulting from reductions in sarcoplasmic reticulum calcium uptake current, in a strongly coupled electromechnical model of the failing human myocyte. Our results demonstrate that the magnitude of FORCE-ALT is largest at clinically relevant pacing rates (<110 bpm), where APV-ALT was smallest. The magnitudes of FORCE-ALTM, CA-ALTM and APV-ALTM were dependent on pacing rate. Due to myofilament feedback, the magnitude of the alternans was also dependent on sarcomere length, and on the level of heart failure induced-remodeling of mechanical parameters involved in thin filament regulation. These findings provide important insight into the cellular mechanisms underlying pressure alternans at clinically relevant pacing rates (<110 bpm) and may aid in investigating whether pressure alternans is an improved and reliable predictor of propensity for ventricular arrhythmias in human heart failure.

Acknowledgments

The authors thank Dr. Jason Bayer, University of Bordeaux, and Robert Blake, Johns Hopkins University, for their valuable assistance in this study. This research was supported by National Institute of Health grants numbers R01 HL103428 and DP1 HL123271, and National Science Foundation grant number IOS-1124804 to Dr. Trayanova and by the David C. Gakenheimer Fellowship to Melanie Zile.

Abbreviations

APV-ALT	action potential voltage alternans
APV-ALTM	action potential voltage alternans magnitude
$[Ca]_i$	free intracellular calcium concentration
CA-ALT	$[Ca]_i$ alternans
CA-ALTM	$[Ca]_i$ alternans magnitude
CL	cycle length
$[Ca]_{Troponin}$	total calcium bound to Troponin C
FORCE-ALT	active force alternans
FORCE-ALTM	active force alternans magnitude
RU	regulatory unit
SL	sarcomere length
XB	crossbridge

References

Ambardekar AV, Walker JS, Walker LA, Cleveland JC Jr, Lowes BD, Buttrick PM. Incomplete recovery of myocyte contractile function despite improvement of myocardial architecture with left ventricular assist device support. Circ Heart Fail. 2011; 4:425–32. [PubMed: 21540356]

Bardy GH, Lee KL, Mark DB, Poole JE, Packer DL, Boineau R, Domanski M, Troutman C, Anderson J, Johnson G, McNulty SE, Clapp-Channing N, Davidson-Ray LD, Fraulo ES, Fishbein DP, Luceri RM, Ip JH. Amiodarone or an implantable cardioverter-defibrillator for congestive heart failure. N Engl J Med. 2005; 352:225–37. [PubMed: 15659722]

Bayer JD, Narayan SM, Lalani GG, Trayanova NA. Rate-dependent action potential alternans in human heart failure implicates abnormal intracellular calcium handling. Heart Rhythm. 2010; 7:1093–101. [PubMed: 20382266]

Belin RJ, Sumandea MP, Allen EJ, Schoenfelt K, Wang H, Solaro RJ, de Tombe PP. Augmented protein kinase C-alpha-induced myofilament protein phosphorylation contributes to myofilament dysfunction in experimental congestive heart failure. Circ Res. 2007; 101:195–204. [PubMed: 17556659]

Belin RJ, Sumandea MP, Kobayashi T, Walker LA, Rundell VL, Urboniene D, Yuzhakova M, Ruch SH, Geenen DL, Solaro RJ, de Tombe PP. Left ventricular myofilament dysfunction in rat experimental hypertrophy and congestive heart failure. Am J Physiol Heart Circ Physiol. 2006; 291:H2344–53. [PubMed: 16815982]

Berger RD, Kasper EK, Baughman KL, Marban E, Calkins H, Tomaselli GF. Beat-to-beat QT interval variability: novel evidence for repolarization lability in ischemic and nonischemic dilated cardiomyopathy. Circulation. 1997; 96:1557–65. [PubMed: 9315547]

Bloomfield DM, Bigger JT, Steinman RC, Namerow PB, Parides MK, Curtis AB, Kaufman ES, Davidenko JM, Shinn TS, Fontaine JM. Microvolt T-wave alternans and the risk of death or sustained ventricular arrhythmias in patients with left ventricular dysfunction. J Am Coll Cardiol. 2006; 47:456–63. [PubMed: 16412877]

Brooks WW, Bing OH, Litwin SE, Conrad CH, Morgan JP. Effects of treppe and calcium on intracellular calcium and function in the failing heart from the spontaneously hypertensive rat. Hypertension. 1994; 24:347–56. [PubMed: 8082941]

Chen X, Hu Y, Fetics BJ, Berger RD, Trayanova NA. Unstable QT interval dynamics precedes ventricular tachycardia onset in patients with acute myocardial infarction: a novel approach to

detect instability in QT interval dynamics from clinical ECG. Circ Arrhythm Electrophysiol. 2011; 4:858–66. [PubMed: 21841208]

Chen X, Tereshchenko LG, Berger RD, Trayanova NA. Arrhythmia risk stratification based on QT interval instability: an intracardiac electrocardiogram study. Heart Rhythm. 2013; 10:875–80. [PubMed: 23416373]

Chen X, Trayanova NA. A novel methodology for assessing the bounded-input bounded-output instability in QT interval dynamics: application to clinical ECG with ventricular tachycardia. IEEE Trans Biomed Eng. 2012; 59:2111–7. [PubMed: 21984490]

Couderc JP, Zareba W, McNitt S, Maison-Blanche P, Moss AJ. Repolarization variability in the risk stratification of MADIT II patients. Europace. 2007; 9:717–23. [PubMed: 17639070]

Coulton AT, Stelzer JE. Cardiac myosin binding protein C and its phosphorylation regulate multiple steps in the cross-bridge cycle of muscle contraction. Biochemistry. 2012; 51:3292–301. [PubMed: 22458937]

Cutler MJ, Rosenbaum DS. Risk stratification for sudden cardiac death: is there a clinical role for T wave alternans? Heart Rhythm. 2009; 6:S56–61. [PubMed: 19631909]

Das MK, Khan B, Jacob S, Kumar A, Mahenthiran J. Significance of a fragmented QRS complex versus a Q wave in patients with coronary artery disease. Circulation. 2006; 113:2495–501. [PubMed: 16717150]

de Oliveira BL, Rocha BM, Barra LP, Toledo EM, Sundnes J, Weber dos Santos R. Effects of deformation on transmural dispersion of repolarization using in silico models of human left ventricular wedge. Int J Numer Method Biomed Eng. 2013; 29:1323–37. [PubMed: 23794390]

de Waard MC, van der Velden J, Bito V, Ozdemir S, Biesmans L, Boontje NM, Dekkers DH, Schoonderwoerd K, Schuurbiers HC, de Crom R, Stienen GJ, Sipido KR, Lamers JM, Duncker DJ. Early exercise training normalizes myofilament function and attenuates left ventricular pump dysfunction in mice with a large myocardial infarction. Circ Res. 2007; 100:1079–88. [PubMed: 17347478]

El-Armouche A, Pohlmann L, Schlossarek S, Starbatty J, Yeh YH, Nattel S, Dobrev D, Eschenhagen T, Carrier L. Decreased phosphorylation levels of cardiac myosin-binding protein-C in human and experimental heart failure. J Mol Cell Cardiol. 2007; 43:223–9. [PubMed: 17560599]

Flashman E, Redwood C, Moolman-Smook J, Watkins H. Cardiac myosin binding protein C: its role in physiology and disease. Circ Res. 2004; 94:1279–89. [PubMed: 15166115]

Goldberger JJ, Buxton AE, Cain M, Costantini O, Exner DV, Knight BP, Lloyd-Jones D, Kadish AH, Lee B, Moss A, Myerburg R, Olgin J, Passman R, Rosenbaum D, Stevenson W, Zareba W, Zipes DP. Risk stratification for arrhythmic sudden cardiac death: identifying the roadblocks. Circulation. 2011; 123:2423–30. [PubMed: 21632516]

Gordon AM, Huxley AF, Julian FJ. The variation in isometric tension with sarcomere length in vertebrate muscle fibres. J Physiol. 1966; 184:170–92. [PubMed: 5921536]

Hasenfuss G, Reinecke H, Studer R, Meyer M, Pieske B, Holtz J, Holubarsch C, Posival H, Just H, Drexler H. Relation between myocardial function and expression of sarcoplasmic reticulum Ca(2+)-ATPase in failing and nonfailing human myocardium. Circ Res. 1994; 75:434–42. [PubMed: 8062417]

Hirashiki A, Izawa H, Cheng XW, Unno K, Ohshima S, Murohara T. Dobutamine-induced mechanical alternans is a marker of poor prognosis in idiopathic dilated cardiomyopathy. Clin Exp Pharmacol Physiol. 2010; 37:1004–9. [PubMed: 20626415]

Hirashiki A, Izawa H, Somura F, Obata K, Kato T, Nishizawa T, Yamada A, Asano H, Ohshima S, Noda A, Iino S, Nagata K, Okumura K, Murohara T, Yokota M. Prognostic value of pacing-induced mechanical alternans in patients with mild-to-moderate idiopathic dilated cardiomyopathy in sinus rhythm. J Am Coll Cardiol. 2006; 47:1382–9. [PubMed: 16580526]

Hohnloser SH, Ikeda T, Cohen RJ. Evidence regarding clinical use of microvolt T-wave alternans. Heart Rhythm. 2009; 6:S36–44. [PubMed: 19168396]

Ito M, Kodama M, Kashimura T, Obata H, Mitsuma W, Hirono S, Tomita M, Ohno Y, Tanabe N, Aizawa Y. Comparison of patients with pulmonary arterial hypertension with versus without right-sided mechanical alternans. Am J Cardiol. 2012; 109:428–31. [PubMed: 22071213]

Ji YC, Gray RA, Fenton FH. Implementation of Contraction to Electrophysiological Ventricular Myocyte Models, and Their Quantitative Characterization via Post-Extrasystolic Potentiation. PLoS One. 2015; 10:e0135699. [PubMed: 26317204]

Kashimura T, Kodama M, Tanaka K, Sonoda K, Watanabe S, Ohno Y, Tomita M, Obata H, Mitsuma W, Ito M, Hirono S, Hanawa H, Aizawa Y. Mechanical alternans in human idiopathic dilated cardiomyopathy is caused with impaired force-frequency relationship and enhanced poststimulation potentiation. Heart Vessels. 2013; 28:336–44. [PubMed: 22573070]

Kashimura T, Kodama M, Watanabe T, Tanaka K, Hayashi Y, Ohno Y, Obata H, Ito M, Hirono S, Hanawa H, Minamino T. Relative refractoriness of left ventricular contraction underlies human tachycardia-induced mechanical and electrical alternans. Pacing Clin Electrophysiol. 2014; 37:197–206. [PubMed: 24025150]

Kihara Y, Morgan JP. Abnormal Cai2+ handling is the primary cause of mechanical alternans: study in ferret ventricular muscles. Am J Physiol. 1991; 261:H1746–55. [PubMed: 1750531]

Kim R, Cingolani O, Wittstein I, McLean R, Han L, Cheng K, Robinson E, Brinker J, Schulman SS, Berger RD, Henrikson CA, Tereshchenko LG. Mechanical alternans is associated with mortality in acute hospitalized heart failure: prospective mechanical alternans study (MAS). Circ Arrhythm Electrophysiol. 2014; 7:259–66. [PubMed: 24585716]

Kockskamper J, Blatter LA. Subcellular Ca2+ alternans represents a novel mechanism for the generation of arrhythmogenic Ca2+ waves in cat atrial myocytes. J Physiol. 2002; 545:65–79. [PubMed: 12433950]

Kodama M, Kato K, Hirono S, Okura Y, Hanawa H, Ito M, Fuse K, Shiono T, Watanabe K, Aizawa Y. Mechanical alternans in patients with chronic heart failure. J Card Fail. 2001; 7:138–45. [PubMed: 11420765]

Kotsanas G, Holroyd SM, Young R, Gibbs CL. Mechanisms contributing to pulsus alternans in pressure-overload cardiac hypertrophy. Am J Physiol. 1996; 271:H2490–500. [PubMed: 8997309]

Kuchar DL, Thorburn CW, Sammel NL. Prediction of serious arrhythmic events after myocardial infarction: signal-averaged electrocardiogram, Holter monitoring and radionuclide ventriculography. J Am Coll Cardiol. 1987; 9:531–8. [PubMed: 3819200]

Lab MJ, Lee JA. Changes in intracellular calcium during mechanical alternans in isolated ferret ventricular muscle. Circ Res. 1990; 66:585–95. [PubMed: 2306800]

Lamberts RR, Hamdani N, Soekhoe TW, Boontje NM, Zaremba R, Walker LA, de Tombe PP, van der Velden J, Stienen GJ. Frequency-dependent myofilament Ca2+ desensitization in failing rat myocardium. J Physiol. 2007; 582:695–709. [PubMed: 17478529]

Lee HC, Mohabir R, Smith N, Franz MR, Clusin WT. Effect of ischemia on calcium-dependent fluorescence transients in rabbit hearts containing indo 1. Correlation with monophasic action potentials and contraction. Circulation. 1988; 78:1047–59. [PubMed: 2844438]

Levine RJ, Kensler RW, Yang Z, Stull JT, Sweeney HL. Myosin light chain phosphorylation affects the structure of rabbit skeletal muscle thick filaments. Biophys J. 1996; 71:898–907. [PubMed: 8842229]

Lloyd-Jones D, Adams R, Carnethon M, De Simone G, Ferguson TB, Flegal K, Ford E, Furie K, Go A, Greenlund K, Haase N, Hailpern S, Ho M, Howard V, Kissela B, Kittner S, Lackland D, Lisabeth L, Marelli A, McDermott M, Meigs J, Mozaffarian D, Nichol G, O'Donnell C, Roger V, Rosamond W, Sacco R, Sorlie P, Stafford R, Steinberger J, Thom T, Wasserthiel-Smoller S, Wong N, Wylie-Rosett J, Hong Y. Heart disease and stroke statistics--2009 update: a report from the American Heart Association Statistics Committee and Stroke Statistics Subcommittee. Circulation. 2009; 119:480–6. [PubMed: 19171871]

Messer AE, Jacques AM, Marston SB. Troponin phosphorylation and regulatory function in human heart muscle: dephosphorylation of Ser23/24 on troponin I could account for the contractile defect in end-stage heart failure. J Mol Cell Cardiol. 2007; 42:247–59. [PubMed: 17081561]

Moss RL, Fitzsimons DP. Myosin light chain 2 into the mainstream of cardiac development and contractility. Circ Res. 2006; 99:225–7. [PubMed: 16888245]

Mulieri LA, Hasenfuss G, Leavitt B, Allen PD, Alpert NR. Altered myocardial force-frequency relation in human heart failure. Circulation. 1992; 85:1743–50. [PubMed: 1572031]

Narayan SM. T-wave alternans and the susceptibility to ventricular arrhythmias. J Am Coll Cardiol. 2006; 47:269–81. [PubMed: 16412847]

Narayan SM, Bayer JD, Lalani G, Trayanova NA. Action potential dynamics explain arrhythmic vulnerability in human heart failure: a clinical and modeling study implicating abnormal calcium handling. J Am Coll Cardiol. 2008; 52:1782–92. [PubMed: 19022157]

Narayan SM, Franz MR, Lalani G, Kim J, Sastry A. T-wave alternans, restitution of human action potential duration, and outcome. J Am Coll Cardiol. 2007; 50:2385–92. [PubMed: 18154963]

Olsson MC, Patel JR, Fitzsimons DP, Walker JW, Moss RL. Basal myosin light chain phosphorylation is a determinant of Ca2+ sensitivity of force and activation dependence of the kinetics of myocardial force development. Am J Physiol Heart Circ Physiol. 2004; 287:H2712–8. [PubMed: 15331360]

Orchard CH, McCall E, Kirby MS, Boyett MR. Mechanical alternans during acidosis in ferret heart muscle. Circ Res. 1991; 68:69–76. [PubMed: 1984873]

Pastore JM, Girouard SD, Laurita KR, Akar FG, Rosenbaum DS. Mechanism linking T-wave alternans to the genesis of cardiac fibrillation. Circulation. 1999; 99:1385–94. [PubMed: 10077525]

Patel JR, Diffee GM, Huang XP, Moss RL. Phosphorylation of myosin regulatory light chain eliminates force-dependent changes in relaxation rates in skeletal muscle. Biophys J. 1998; 74:360–8. [PubMed: 9449336]

Pieske B, Sutterlin M, Schmidt-Schweda S, Minami K, Meyer M, Olschewski M, Holubarsch C, Just H, Hasenfuss G. Diminished post-rest potentiation of contractile force in human dilated cardiomyopathy. Functional evidence for alterations in intracellular Ca2+ handling. J Clin Invest. 1996; 98:764–76. [PubMed: 8698869]

Qu Z, Xie Y, Garfinkel A, Weiss JN. T-wave alternans and arrhythmogenesis in cardiac diseases. Front Physiol. 2010; 1:154. [PubMed: 21286254]

Rice JJ, Wang F, Bers DM, de Tombe PP. Approximate model of cooperative activation and crossbridge cycling in cardiac muscle using ordinary differential equations. Biophys J. 2008; 95:2368–90. [PubMed: 18234826]

Rosenbaum DS, Jackson LE, Smith JM, Garan H, Ruskin JN, Cohen RJ. Electrical alternans and vulnerability to ventricular arrhythmias. N Engl J Med. 1994; 330:235–41. [PubMed: 8272084]

Schmidt U, Hajjar RJ, Kim CS, Lebeche D, Doye AA, Gwathmey JK. Human heart failure: cAMP stimulation of SR Ca(2+)-ATPase activity and phosphorylation level of phospholamban. Am J Physiol. 1999; 277:H474–80. [PubMed: 10444471]

Selvaraj RJ, Suszko A, Subramanian A, Mak S, Wainstein R, Chauhan VS. Microscopic systolic pressure alternans in human cardiomyopathy: noninvasive evaluation of a novel risk marker and correlation with microvolt T-wave alternans. Heart Rhythm. 2011; 8:236–43. [PubMed: 20950712]

Shkryl VM, Maxwell JT, Domeier TL, Blatter LA. Refractoriness of sarcoplasmic reticulum Ca2+ release determines Ca2+ alternans in atrial myocytes. Am J Physiol Heart Circ Physiol. 2012; 302:H2310–20. [PubMed: 22467301]

ten Tusscher KH, Noble D, Noble PJ, Panfilov AV. A model for human ventricular tissue. Am J Physiol Heart Circ Physiol. 2004; 286:H1573–89. [PubMed: 14656705]

ten Tusscher KH, Panfilov AV. Alternans and spiral breakup in a human ventricular tissue model. Am J Physiol Heart Circ Physiol. 2006; 291:H1088–100. [PubMed: 16565318]

Trayanova NA, Rice JJ. Cardiac electromechanical models: from cell to organ. Front Physiol. 2011; 2:43. [PubMed: 21886622]

van der Velden J, de Jong JW, Owen VJ, Burton PB, Stienen GJ. Effect of protein kinase A on calcium sensitivity of force and its sarcomere length dependence in human cardiomyocytes. Cardiovasc Res. 2000; 46:487–95. [PubMed: 10912459]

van Der Velden J, Klein LJ, Zaremba R, Boontje NM, Huybregts MA, Stooker W, Eijsman L, de Jong JW, Visser CA, Visser FC, Stienen GJ. Effects of calcium, inorganic phosphate, and pH on isometric force in single skinned cardiomyocytes from donor and failing human hearts. Circulation. 2001; 104:1140–6. [PubMed: 11535570]

van der Velden J, Narolska NA, Lamberts RR, Boontje NM, Borbely A, Zaremba R, Bronzwaer JG, Papp Z, Jaquet K, Paulus WJ, Stienen GJ. Functional effects of protein kinase C-mediated

myofilament phosphorylation in human myocardium. Cardiovasc Res. 2006; 69:876–87. [PubMed: 16376870]

van der Velden J, Papp Z, Boontje NM, Zaremba R, de Jong JW, Janssen PM, Hasenfuss G, Stienen GJ. The effect of myosin light chain 2 dephosphorylation on Ca2+-sensitivity of force is enhanced in failing human hearts. Cardiovasc Res. 2003a; 57:505–14. [PubMed: 12566123]

van der Velden J, Papp Z, Zaremba R, Boontje NM, de Jong JW, Owen VJ, Burton PB, Goldmann P, Jaquet K, Stienen GJ. Increased Ca2+-sensitivity of the contractile apparatus in end-stage human heart failure results from altered phosphorylation of contractile proteins. Cardiovasc Res. 2003b; 57:37–47. [PubMed: 12504812]

Weiss JN, Karma A, Shiferaw Y, Chen PS, Garfinkel A, Qu Z. From pulsus to pulseless: the saga of cardiac alternans. Circ Res. 2006; 98:1244–53. [PubMed: 16728670]

Wolff MR, Buck SH, Stoker SW, Greaser ML, Mentzer RM. Myofibrillar calcium sensitivity of isometric tension is increased in human dilated cardiomyopathies: role of altered beta-adrenergically mediated protein phosphorylation. J Clin Invest. 1996; 98:167–76. [PubMed: 8690789]

Wolff MR, Whitesell LF, Moss RL. Calcium sensitivity of isometric tension is increased in canine experimental heart failure. Circ Res. 1995; 76:781–9. [PubMed: 7728995]

Xie W, Santulli G, Guo X, Gao M, Chen BX, Marks AR. Imaging atrial arrhythmic intracellular calcium in intact heart. J Mol Cell Cardiol. 2013; 64:120–3. [PubMed: 24041536]

Zaremba R, Merkus D, Hamdani N, Lamers JM, Paulus WJ, Dos Remedios C, Duncker DJ, Stienen GJ, van der Velden J. Quantitative analysis of myofilament protein phosphorylation in small cardiac biopsies. Proteomics Clin Appl. 2007; 1:1285–90. [PubMed: 21136625]

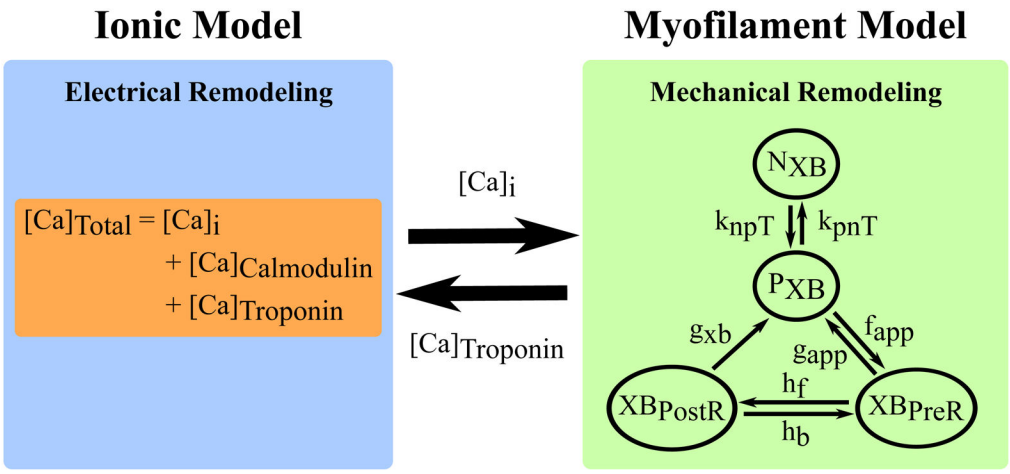

Figure 1.

Strongly Coupled Human Electromechanical Myocyte Model with myofilament feedback via $[Ca]_{Troponin}$. A modified version of the Markov state diagram of the myofilament model from Rice *et al*, which describes the activation of the thin filament by intracellular calcium binding to Troponin C as well as thin filament binding to thick filament crossbridges (XBs), is shown. The transition rates (k_{npT} and k_{pnT}) between the thin filament states where XB formation is inhibited (N_{XB}) and where weakly bound XB formation is possible (P_{XB}) are both functions of $perm_{50}$, k_{on}, k_{offH}, and k_{offL}. The rate k_{npT} is also dependent on k_{n_p}, and k_{pnT} is additionally dependent on k_{p_n}. The XB_{PreR} and XB_{PostR} states represent a thin filament with a strongly bound XB that do not and do, respectively, have rotated myosin heads which induced strain (Rice et al., 2008).

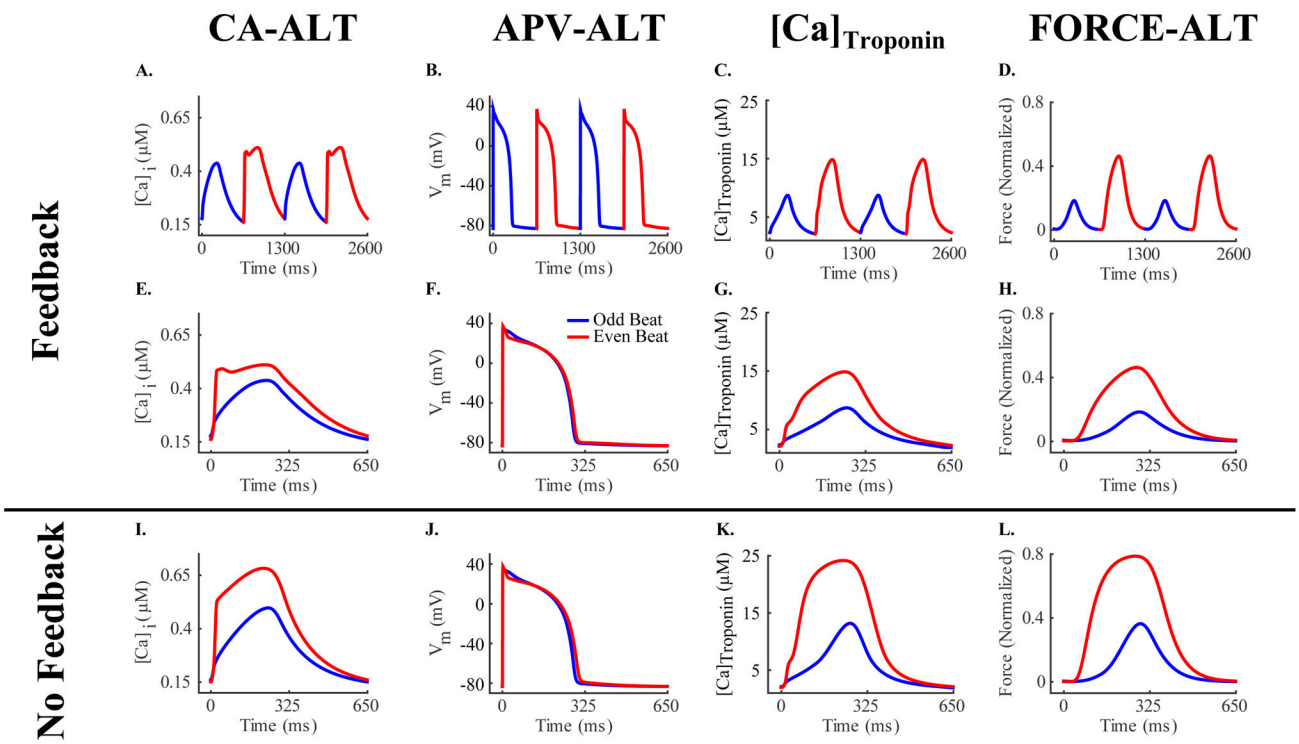

Figure 2.

CA-ALT (column 1), APV-ALT (column 2), $[Ca]_{Troponin}$ (column 3), and FORCE-ALT (column 4) for simulations incorporating electrical remodeling in the absence of mechanical remodeling for a pacing CL of 650 ms and for SL=2.1 μm. Alternans are plotted over time in row 1 showing that CA-ALT was sufficient to produce APV-ALT, $[Ca]_{Troponin}$ alternans, and FORCE-ALT. Odd (blue) and even (red) beats from row 1 are superimposed to illustrate that the magnitude of alternans in rows 2 (strongly coupled simulations) and 3 (weakly coupled simulations) were different with and without myofilament feedback.

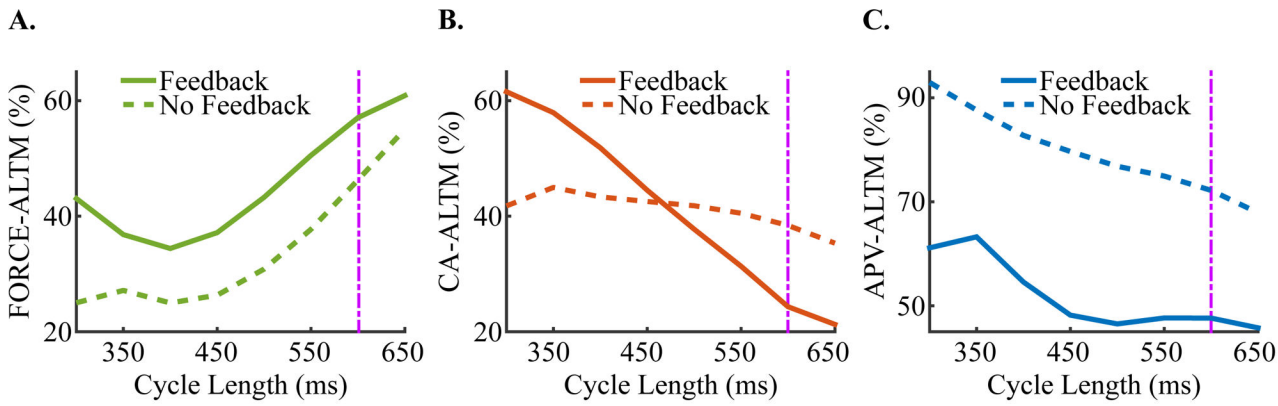

Figure 3.

Dependence of FORCE-ALTM (A), CA-ALTM (B), and APV-ALTM (C) to CL in simulations with electrical remodeling in the absence of mechanical remodeling at SL=2.1 μm for both the strongly (solid lines) and weakly coupled (dashed lines) models. The purple dashpot line indicates where the data in Figure 4 are taken from (CL=600 ms). No alternans occurred for pacing CLs>650 ms for either the strongly or weakly coupled model.

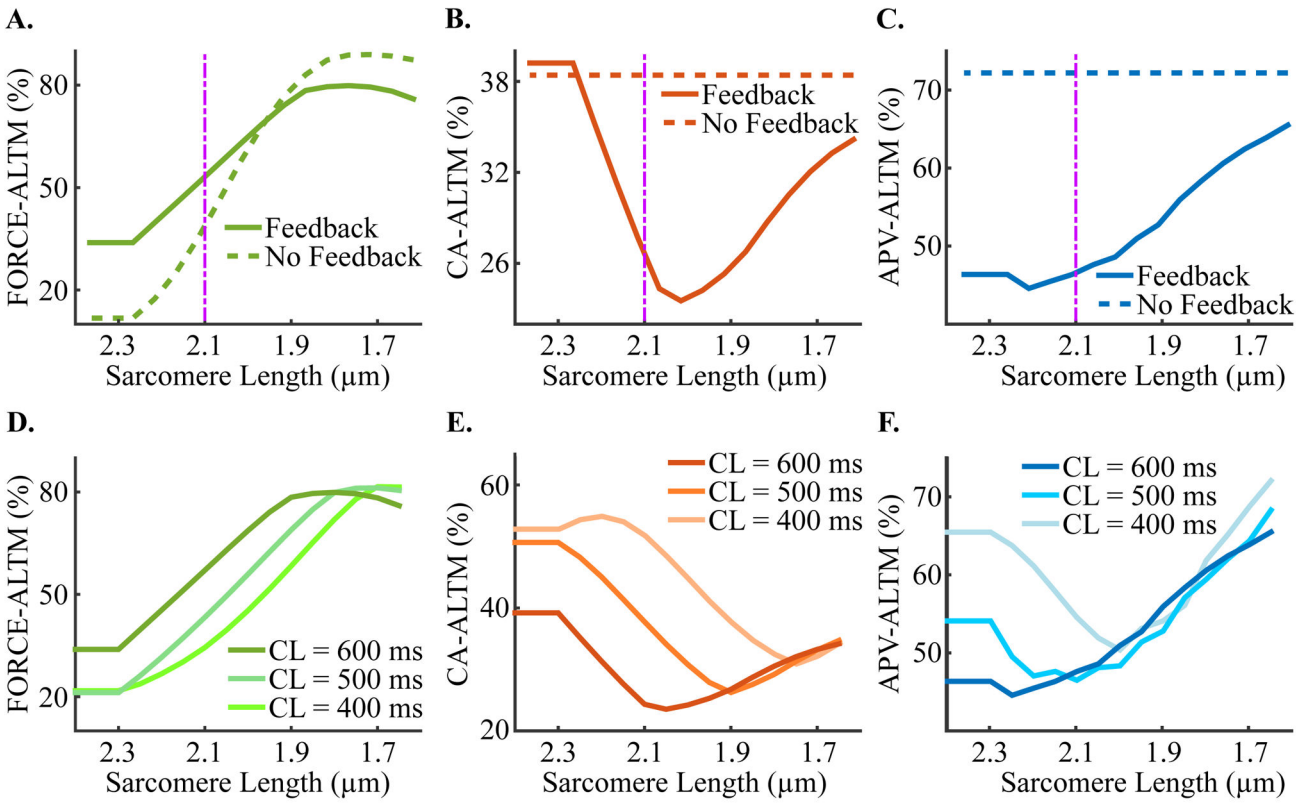

Figure 4.

Sensitivity of FORCE-ALTM (A), CA-ALTM (B), and APV-ALTM (C) to SL in simulations with electrical remodeling in the absence of mechanical remodeling at CL=600 ms for both the strongly (solid lines) and weakly (dashed lines) coupled models. Plots of the dependence of FORCE-ALTM (D), CA-ALTM (E), and APV-ALTM (F) on SL are shown for slow and fast pacing rates for the strongly coupled model. The purple dashpot line indicates where the data displayed in Figure 3 are from (SL=2.1 μm).

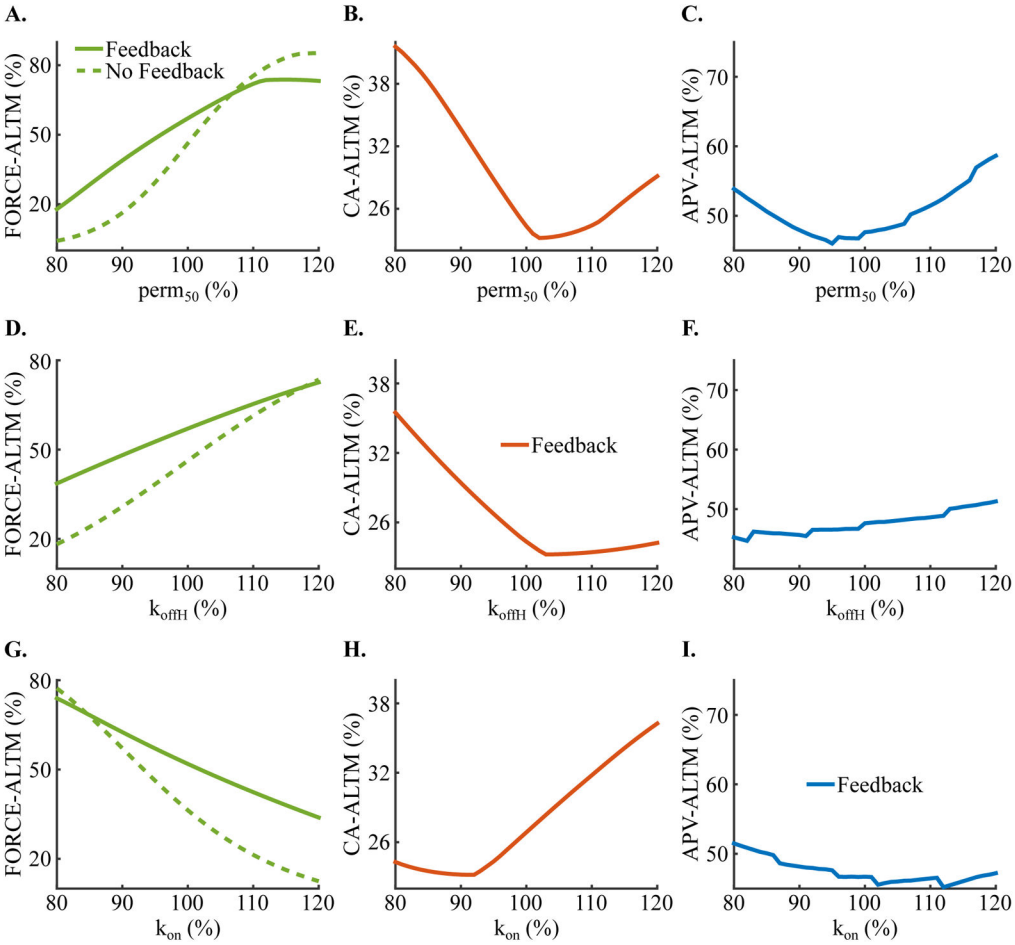

Figure 5.

Dependence of FORCE-ALTM (column 1), CA-ALTM (column 2), and APV-ALTM (column 3) on the level of mechanical remodeling for pacing CL=600 ms and SL=2.1 μm for the strongly coupled model (solid lines). Dashed line in the FORCE-ALTM refers to the weakly coupled model. Heart-failure remodeling mechanical parameters $perm_{50}$ (row 1), k_{offH} (row 2), and k_{on} (row 3), are displayed as a percent of their normal values.

Table 1

Control and Heart Failure values for important model parameters. I_{up} is from the ten Tusscher *et al* ionic model (ten Tusscher and Panfilov, 2006). All other parameters are from the Rice *et al* myofilament model (Rice et al., 2008).

Parameter	Control Value (CV)	Heart Failure Value	Effect of HF remodeling on Alternans
I_{up}	0.006375 mM/ms	**CV*27%**	**Required for alternans to occur**
$perm_{50}$	0.5 (unitless)	Range of Values (Increments of 1%): **CV*80% to CV*120%**	**Largest** effect on alternans magnitude
k_{on}	47.5 1/μMs		**Large** effect on alternans magnitude
k_{offH}	25 1/s		**Large** effect on alternans magnitude
k_{offL}	250 1/s		Negligible effects on alternans magnitude
k_{n_p}	0.61 1/ms		
k_{p_n}	0.016 1/ms		
f_{app}	4.8 1/ms		
g_{app}	0.093 1/ms		
h_f	0.010 1/ms		
h_b	0.035 1/ms		
g_{xb}	0.030 1/ms		